**The EMBO Journal (2007) 26,** 2169–2179 | © 2007 European Molecular Biology Organization | All Rights Reserved 0261-4189/07
www.embojournal.org

THE EMBO JOURNAL

# Cajal bodies and the nucleolus are required for a plant virus systemic infection

**Sang Hyon Kim[1], Eugene V Ryabov[2], Natalia O Kalinina[1,3], Daria V Rakitina[1,3], Trudi Gillespie[1], Stuart MacFarlane[1], Sophie Haupt[4], John WS Brown[1] and Michael Taliansky[1,*]**

[1]Scottish Crop Research Institute, Invergowrie, Dundee, UK, [2]HRI, University of Warwick, Wellesbourne, Warwick, UK, [3]AN Belozersky Institute of Physico-Chemical Biology, Moscow State University, Moscow, Russia and [4]School of Life Sciences, University of Dundee, Dundee, UK

**The nucleolus and Cajal bodies (CBs) are prominent interacting subnuclear domains involved in a number of crucial aspects of cell function. Certain viruses interact with these compartments but the functions of such interactions are largely uncharacterized. Here, we show that the ability of the groundnut rosette virus open reading frame (ORF) 3 protein to move viral RNA long distances through the phloem strictly depends on its interaction with CBs and the nucleolus. The ORF3 protein targets and reorganizes CBs into multiple CB-like structures and then enters the nucleolus by causing fusion of these structures with the nucleolus. The nucleolar localization of the ORF3 protein is essential for subsequent formation of viral ribonucleoprotein (RNP) particles capable of virus long-distance movement and systemic infection. We provide a model whereby the ORF3 protein utilizes trafficking pathways involving CBs to enter the nucleolus and, along with fibrillarin, exit the nucleus to form viral 'transport-competent' RNP particles in the cytoplasm.**

*The EMBO Journal* (2007) **26,** 2169–2179. doi:10.1038/sj.emboj.7601674; Published online 5 April 2007
*Subject Categories*: plant biology; microbiology & pathogens
*Keywords*: Cajal bodies; nucleolus; ribonucleoprotein particles; umbravirus

## Introduction

The nucleolus is a prominent subnuclear domain and is the site of transcription of rRNA, processing of pre-rRNAs and biogenesis of preribosomal particles. In addition, the nucleolus also participates in other aspects of RNA processing and cell function such as stress responses and the cell cycle (Rubbi and Milner, 2003; Olsen, 2004). The nucleolus is structurally and functionally linked to Cajal bodies (CBs) that are conserved structures found in both animals and plants (Beven *et al*, 1995; Cioce and Lamond, 2005). CBs contain small nuclear and small nucleolar ribonucleoprotein particles (snRNPs and snoRNPs) as well as a range of different proteins including coilin, a protein essential for CB formation, and some nucleolar proteins such as fibrillarin, dyskerin and Nopp140 (Ogg and Lamond, 2002; Cioce and Lamond, 2005; Matera and Shpargel, 2006). They are involved in the maturation of spliceosomal snRNPs and snoRNPs where newly assembled snRNPs and snoRNPs traffick through CBs before accumulating in splicing speckles and the nucleolus, respectively (Sleeman and Lamond, 1999; Sleeman *et al*, 2001). CBs are dynamic structures that can move within the nucleus and interact with chromatin and the loci of specific genes (Boudonck *et al*, 1999; Platani *et al*, 2002). The multifunctional nature of the nucleolus and CBs has recently been extended to RNA silencing: in *Arabidopsis*, the production of heterochromatic small interfering RNAs involved in transcriptional silencing occurs in CBs or processing foci in the nucleolus (Li *et al*, 2006; Pontes *et al*, 2006). Finally, a number of animal and plant viruses including the RNA-containing tobacco etch virus and the DNA-containing tomato yellow leaf curl virus have a nucleolar phase in their life cycles (see Hiscox, 2002, 2007 for reviews). However, the specific role of the nucleolus and other subnuclear bodies in virus infections remains elusive.

Umbraviruses differ from most other viruses in that they do not encode a capsid protein (CP) such that conventional virus particles are not formed in infected plants. Umbraviral genomes encode at least three proteins (Figure 1A). In the umbravirus, groundnut rosette virus (GRV), two open reading frames (ORFs) at the 5′-end of the RNA are expressed by a frameshift mechanism as a single protein that appears to be an RNA replicase (Figure 1A; Taliansky and Robinson, 2003). The other ORFs (ORF3 and ORF4) overlap with each other. ORF4 encodes the movement protein that mediates the cell-to-cell movement of viral RNA via plasmodesmata (Ryabov *et al*, 1998). ORF3 protein is the long-distance movement factor that facilitates trafficking of viral RNA through the phloem, the specialized vascular system used by plants for the transport of assimilates and macromolecules (Ryabov *et al*, 1999).

Umbraviral ORF3 proteins (26–29 kDa) show no significant similarity with any other recorded or predicted proteins (Taliansky and Robinson, 2003). The GRV ORF3 protein interacts with viral RNA *in vivo* to form filamentous ribonucleoprotein (RNP) particles, which have elements of regular helical structure, but not the uniformity typical of virus particles (Taliansky *et al*, 2003). The RNPs accumulate in cytoplasmic inclusion bodies, which have been detected in all cell types and, more importantly, were abundant in phloem-associated cells (Taliansky *et al*, 2003). The RNPs protect the viral RNA and move long distances through the phloem, thereby determining the ability of umbravirus to cause systemic infection. Finally, in addition to its presence in the cytoplasm, the ORF3 protein was also found in nuclei and predominantly in nucleoli (Ryabov *et al*, 1998, 2004).

In this paper, we demonstrate that once the GRV ORF3 protein has been imported into the nucleus, it interacts with

*Corresponding author. Plant Pathology, Scottish Crop Research Institute, Invergowrie, Dundee DD2 5DA, UK. Tel.: +44 1382 562731; Fax: +44 1382 562426; E-mail: mtalia@scri.sari.ac.uk

**Received: 25 August 2006; accepted: 13 March 2007; published online: 5 April 2007**

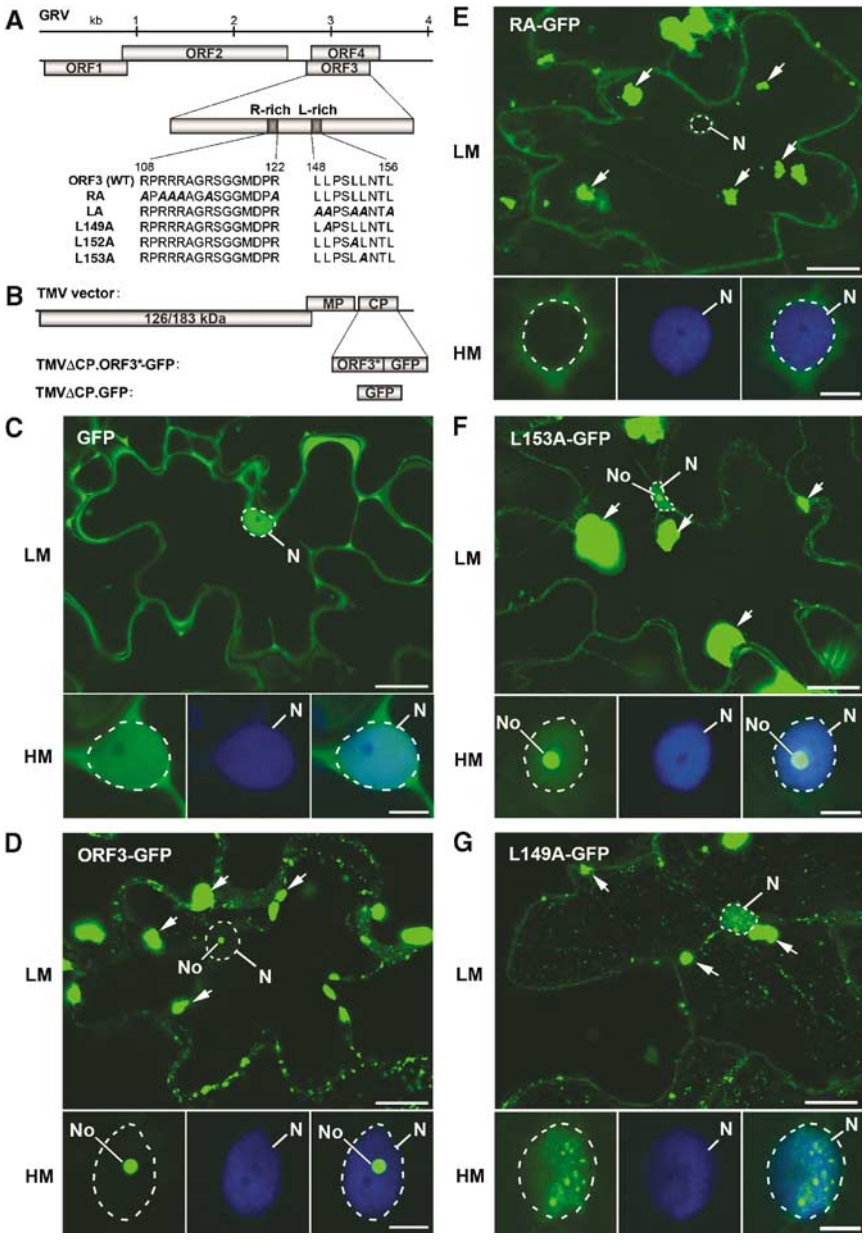


**Figure 1** ORF3 protein domains involved in nuclear localization and cRNP formation. (**A**) Schematic representation of the GRV genome with protein sequences of the wild-type (WT) and mutant ORF3 R- and L-rich domains. (**B**) Representation of the TMV-based vector for expression of WT and mutated ORF3 (ORF3*)-GFP fusion proteins or GFP alone replacing the TMV CP gene. (C–G) Intracellular localization of free GFP (**C**), ORF3-GFP (**D**) and the mutant GFP fusions: RA-GFP (**E**), L153A-GFP (**F**) and L149A-GFP (**G**) expressed from a TMVΔCP vector in epidermal cells and determined by CLSM. Each set of GFP images presents a whole cell at low magnification (LM) and a nucleus at high magnification (HM) showing GFP image (left-hand panel), DAPI staining (centre panel) and overlaid GFP and DAPI images (right-hand panel). Free GFP localizes to the nucleus (largely excluded from the nucleolus) and cytoplasm (C) whereas ORF3-GFP localizes to the nucleolus and cytoplasmic inclusions (indicated by arrows) (D). RA-GFP is largely excluded from the nucleus (E), L153A-GFP is nuclear with strong localization to the nucleolus (F) and L149A-GFP is nuclear with strong accumulation in small nuclear bodies (G). No, nucleolus; N, nucleus (shown by dashed line). Scale bars, 20 μm (LM) and 5 μm (HM).

and reorganizes CBs into multiple CB-like structures (CBLs) and enters the nucleolus by causing fusion of the CBLs with the nucleolus. The ORF3 protein also causes the redistribution of some of the pool of the major nucleolar protein, fibrillarin, to the cytoplasm. More importantly, the nucleolar phase of the ORF3 protein is essential for the formation of viral RNPs and consequently virus long-distance movement, providing a model where CBs and the nucleolus are integrally required for these processes.

## Results

### *Protein domains of ORF3 involved in nuclear localization*

ORF3 proteins from different umbraviruses contain two conserved domains: a basic arginine-rich sequence (positions 108–122; R-rich domain) and a hydrophobic leucine-rich region (amino acids 148–156; L-rich domain) showing invariant leucine residues in a motif 149-LXXLL-153 (Figure 1A)

(Taliansky and Robinson, 2003; Ryabov *et al*, 2004). To examine the effect of these conserved regions on the detailed localization of ORF3 protein, ORF3 constructs were introduced into a tobacco mosaic virus (TMV) vector where the TMV CP (normally essential for virus long-distance movement) had been removed (TMVΔCP). The CP was replaced by a fusion of the ORF3 protein to the N-terminus of GFP (TMVΔCP.ORF3-GFP—abbreviated to ORF3-GFP) (Figure 1B). Following inoculation of *Nicotiana benthamiana* plants, the ORF3-GFP fusion complemented the inability of TMVΔCP to move long distances through the phloem (data not shown).

For localizations, infection sites were allowed to develop on inoculated leaves for about 7 days (late stage of infection in inoculated leaves) before fluorescence was monitored. Free GFP expressed from TMVΔCP (TMVΔCP-GFP) was clearly visible in the nucleus (but largely excluded from the nucleolus) and cytoplasm, which is distributed as a thin layer appressed to the highly convoluted cell wall of the epidermal cells (Figure 1C). In leaves inoculated with ORF3-GFP, the fusion protein localized to the nucleolus and in the vast majority of cells to large cytoplasmic inclusions (Figure 1D). The nucleolar localization is clearly shown in the higher magnification images of individual nuclei below the whole cell image confirming our previous observations obtained by electron microscopy (Ryabov *et al*, 2004) and confocal laser scanning microscopy (Ryabov *et al*, 1998). The fluorescent cytoplasmic inclusions varied in number and size (sometimes as large as 10 μm). The pattern of fluorescence in the inclusions also varied from uniform, intense labelling to diffuse labelling with numerous more heavily labelled speckles (compare ORF3-GFP in Figures 1D and 6A), presumably reflecting different levels of ORF3 protein accumulation in different cells.

Mutations to the R- and L-rich domains were introduced into ORF3-GFP to monitor effects on intracellular localization. Replacement of all six arginine residues (amino-acid positions 108, 110, 111, 112, 115 and 122) in the R-rich domain by alanine residues gave RA-GFP (Figure 1A), which was unable to enter the nucleus (Figure 1E), confirming previous observations that the R-rich domain is involved in nuclear import (Ryabov *et al*, 2004). Fluorescence was also observed in large inclusions in the cytoplasm of infected cells (Figure 1E). None of the single arginine–alanine substitutions affected nucleolar localization of the ORF3 protein or inclusion formation (Figure 3C).

Mutations to the leucine-rich region replaced either all the invariant leucine residues (positions 149, 152 and 153) or individual leucines with alanine residues. Mutation of L152 or L153 did not affect the nucleolar localization of ORF3-GFP but led to a higher accumulation of the protein in the nucleoplasm than was observed with unmutated ORF3-GFP (Figure 1F). On the other hand, replacement of either all three leucines (LA-GFP) or the single leucine L149 (L149A-GFP) caused the mutant fusion proteins to be excluded from the nucleolus and to accumulate in the nucleus in multiple small structures in the nucleoplasm (Figure 1G). Thus, L149A, in addition to the R-rich domain, is essential for nucleolar targeting of the ORF3 protein. The higher level of nuclear accumulation of all of the leucine mutants compared to ORF3-GFP (Figure 1D) suggests that the leucine-rich region acts as a nuclear export signal (Ryabov *et al*, 2004) and that the ORF3 protein traffics between the nucleus (nucleolus) and cytoplasm in infected cells. As with the wild-type ORF3-GFP or RA-GFP mutant large fluorescent cytoplasmic inclusions were found in cells expressing all of the leucine mutants (Figure 1F and G).

### *Viral RNP particles are present only in large cytoplasmic inclusions formed by the wild-type ORF3 protein*

Following expression of GFP-tagged ORF3 and its mutant proteins, fluorescence was observed in large cytoplasmic inclusions. The majority of plant viruses produce cytoplasmic inclusion bodies, reflecting the high level of production of viral RNA and proteins (see Hull, 2002 for review). For GRV, we showed previously by immunogold labelling (IGL) and *in situ* hybridization (ISH) that the cytoplasmic inclusions were composed of filamentous RNP particles (referred to as cytoplasmic RNPs (c-RNP)) containing the ORF3 protein and viral RNA (Taliansky *et al*, 2003). To characterize the large fluorescent cytoplasmic inclusions formed by the TMV-expressed ORF3-GFP construct and its mutants at late stages of infection, we analyzed cells by electron microscopy, IGL and ISH. Healthy palisade mesophyll cells showed the cytoplasm containing protoplasts around the periphery of the central vacuole with a distinct nucleus and nucleolus (Figure 2A). In addition to these normal organelles, cells infected with TMV vector expressing ORF3-GFP showed the presence of X-bodies or viroplasms, large virus-induced amorphous inclusion bodies typical of TMV infection (Esau and Cronshaw, 1967; Hull, 2002) and frequently (but not always) found in the proximity of the nucleus. The X-bodies formed by ORF3-GFP also contained multiple electron-dense cytoplasmic inclusions (e.g., Figure 2A and B; Taliansky *et al*, 2003). Similar multiple inclusions were observed on closer examination of X-bodies formed in cells expressing the RA-GFP and L149A-GFP mutants (Figure 2B). The inclusions varied in size from 300 nm to 4 μm, and as many as 10 μm, separate inclusions could be found in a single cell section (Figure 2A; see also Taliansky *et al*, 2003). Such inclusion bodies were not detected in cells infected with the TMV vector alone or in healthy cells (Figure 2A).

To examine whether the cytoplasmic inclusions contained viral protein and RNA, sections of inclusion bodies from cells expressing ORF3-GFP, RA-GFP and L149A-GFP were analyzed by IGL and ISH. For ORF3-GFP, masses of filamentous structures were observed in the inclusion bodies that were labelled by antibodies against the ORF3 protein (IGL) and by an RNA probe to the ORF3 region of GRV RNA (ISH) (Figure 2C). Thus, the filamentous structures contained both the ORF3 protein and viral RNA, indicative of the formation of viral RNPs. These cytoplasmic filamentous RNP particles (c-RNP) were very similar to the ORF3 RNP complexes formed in GRV infection whose molecular structure was described in detail previously (Taliansky *et al*, 2003). Formation of the c-RNP particles did not depend on the TMV vector background, as they were also formed during native umbravirus (GRV) infection (Supplementary Figure S1A).

On the other hand, the RA-GFP and L149A-GFP mutants showed little structure in the inclusion bodies, contained mutant ORF3 protein (as shown by IGL) but did not contain viral RNA (as shown by ISH) (Figure 2C). Thus, wild-type ORF3 protein generates cytoplasmic inclusions containing

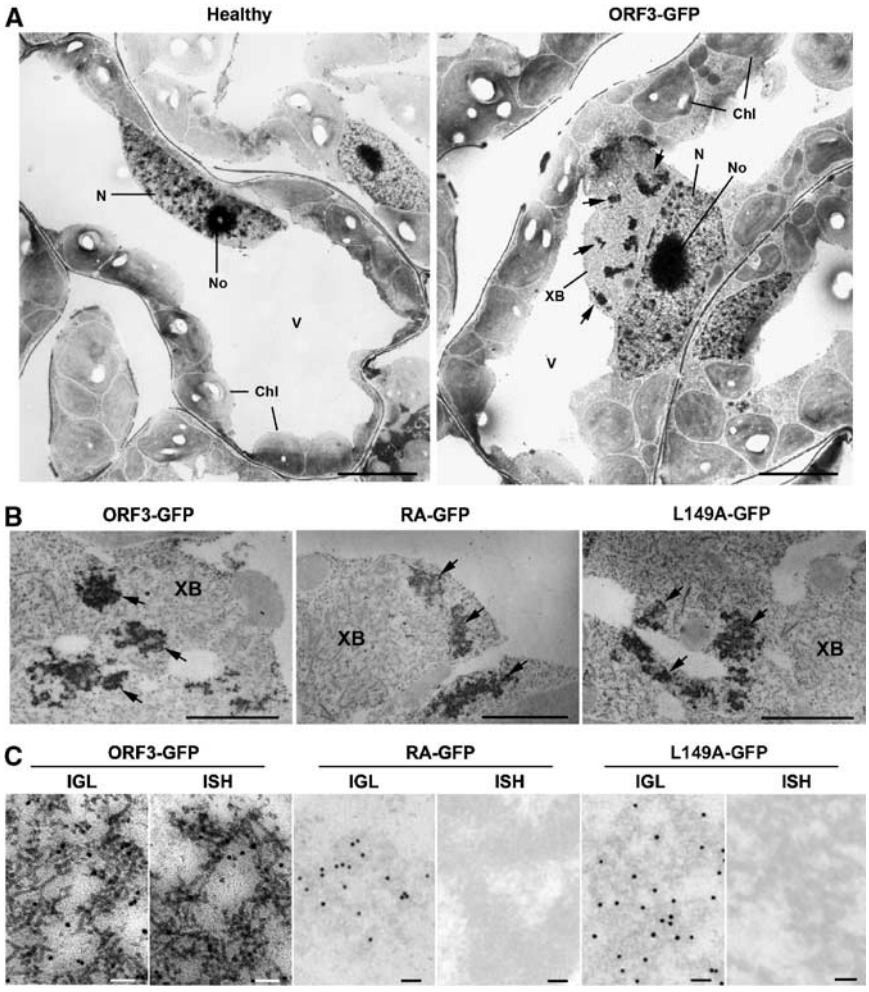


**Figure 2** Electron micrographs showing localization, morphology and structure of inclusions formed by ORF3-GFP or its mutants (RA-GFP and L149A-GFP) in palisade mesophyll cells of *N. benthamiana* plants. (**A**) Sections showing typical general views of healthy cells and cells infected with ORF3-GFP after IGL with antibodies against the ORF3 protein. Cells infected with the ORF3 mutants, RA-GFP and L149A-GFP, are essentially similar. All cells contain normal organelles such as nucleus (N) nucleolus (No), chloroplasts (Chl) and vacuole (V). In addition, virus-infected cells (exemplified by ORF3-GFP) also contain TMV-specific X-bodies (XB) containing electron-dense (gold-labelled) ORF3 protein-related inclusions (shown by arrows). Scale bars, 5 μm. (**B**) Higher magnification of X-bodies and cytoplasmic inclusions of ORF3-GFP and its mutants, RA-GFP and L149A-GFP. XB, X-bodies; arrows, inclusions. Scale bars, 2 μm. (**C**) High-resolution EM sections of cytoplasmic inclusions formed by ORF3-GFP, RA-GFP and L149A-GFP labelled with antibody against the ORF3 protein (IGL) and with an RNA probe specific for the positive strand of the ORF3 gene (ISH). ORF3-GFP inclusions are composed of complexes of filamentous RNP particles (c-RNP) containing the ORF3 protein and viral RNA. The inclusions of the ORF3 mutants, RA-GFP and L149A-GFP did not have a filamentous structure; they contained mutant ORF3 proteins (IGL) but did not contain viral RNA (ISH). All of the inclusions appear as large fluorescence masses (up to 10 μm) in confocal images (Figure 1D–G). Scale bars, 100 nm.

viral RNPs (c-RNP), whereas the amorphous inclusions formed by the ORF3 mutants did not contain viral RNA and, thereby, RNP particles, but only accumulated protein. These cytoplasmic inclusions were, therefore, termed cytoplasmic protein aggregates (c-PAs). In addition to the above mutants, the other leucine mutants also did not produce inclusions with viral RNA/RNPs, forming only ORF3 protein aggregates (c-PA) (data not shown). Thus, although ORF3-GFP and its mutants formed cytoplasmic inclusions, which were readily visible by confocal laser scanning microscopy (Figure 1C–G) and electron microscopy (Figure 2), they differed in their molecular structure and composition, with only the wild-type ORF3-GFP producing viral RNPs (c-RNPs). However, in confocal images (Figure 1D–G), all of the inclusions appear similar as large fluorescent masses in the cytoplasm.

The differences in intracellular localization and ability to form RNP particles among ORF3-GFP and its mutants are unlikely to reflect differences in infectivity (replication and cell-to-cell movement) of the TMV vector or in ORF3 protein accumulation because the size of infection foci and intensity of GFP fluorescence were approximately the same for all constructs (data not shown). The differential localizations also did not depend on the virus vector background as experiments using *Agrobacterium*-mediated transient expression of the corresponding constructs showed similar localization patterns (data not shown).

### *The R- and L-rich domains affect long-distance virus movement*

The TMVΔCP vector does not move rapidly between lower and upper leaves and allows an assessment of whether the

 

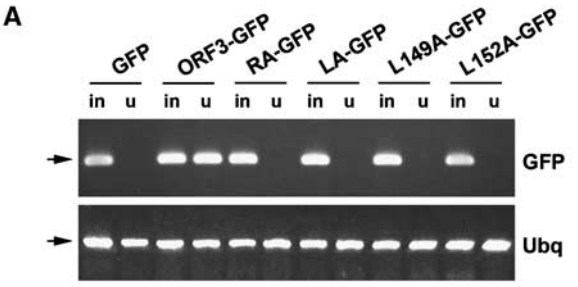


B

| GFP | | ORF3-GFP | | RA-GFP | | LA-GFP | | L149A-GFP | | L152A-GFP | |
|---|---|---|---|---|---|---|---|---|---|---|---|
| in | u | in | u | in | u | in | u | in | u | in | u |
| 46±7 | 0 | 32±8 | 95±7 | 38±6 | 0 | 89±2 | 0 | 41±6 | 0 | 32±6 | 0 |

C

| TMVΔCP constructs | N | No | N-exp | RNP formation | LDM |
|---|---|---|---|---|---|
| ORF3-GFP | + | + | + | + | + |
| RA-GFP | – | – | – | – | – |
| R108A-GFP* | + | + | + | + | + |
| L149A-GFP | + | – | – | – | – |
| LA-GFP | + | – | – | – | – |
| L152A-GFP | + | + | – | – | – |
| L153A-GFP | + | + | – | – | – |

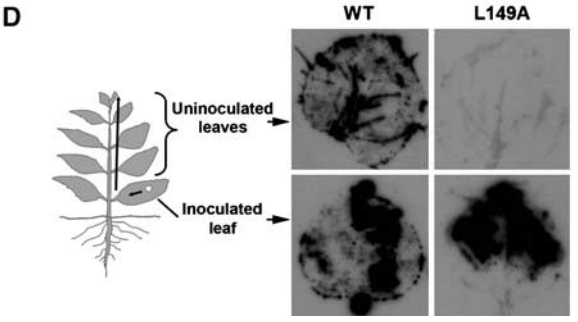


**Figure 3** Protein domains of ORF3 involved in virus long-distance movement. (A, B) Effect of ORF3 protein mutations on the accumulation of TMVΔCP.ORF3 in inoculated (in) and uninoculated (u) leaves of *N. benthamiana* analyzed by RT–PCR (A) and infectivity assay (B). (**A**) Ethidium bromide-stained agarose gels show RT–PCR products (after 50 cycles of amplification) corresponding to fragments of GFP gene (270 bp) and the control ubiquitin gene (176 bp) (indicated by arrows). (**B**) Accumulation of the virus was determined by inoculation of RNA isolated from inoculated (in) and uninoculated (u) leaves on test *N. tabacum* 'Xanthi-nc' plants leading to the production of visible lesions. The data are the average number of lesions per half leaf. Only ORF3-GFP shows the presence of viral RNA (A) and infectious virus (B) in uninoculated leaves of *N. benthamiana*. (**C**) Summary of localization, RNP formation and long-distance movement data showing the correlation between the ability of the ORF3 protein to traffic through the nucleolus to the cytoplasm, its capacity to form viral movement-competent c-RNPs (detected by IGL and ISH, see Figure 2C), and their systemic transport (long-distance movement, LDM). N and No, nuclear and nucleolar localization of the ORF3 protein, respectively; N-exp, nuclear export; LDM, long-distance movement. *, all of the mutants with single arginine–alanine substitutions in the R-rich domain did not affect nuclear localization and c-RNP formation and were able to rescue long-distance virus movement (data not shown) and are exemplified by the R108A-GFP mutant. (**D**) Typical print hybridization patterns of inoculated and uninoculated leaves of *N. benthamiana* infected with PEMV-2 and PEMV-2 containing the L149A mutation in its ORF3. Viral RNA was detected with a $^{32}$P-labelled cDNA probe corresponding to PEMV-2 ORF3.

ORF3 mutants can rescue long-distance movement of TMVΔCP by looking for the spread of ORF3-GFP into uninoculated leaves. ORF3-GFP rescued rapid long-distance movement of TMVΔCP from inoculated to upper uninoculated leaves as shown by the presence of ORF3-GFP RNA in uninoculated leaves (Figure 3A) and the ability of extracts from these leaves to produce infectious lesions on test plants (Figure 3B, summarized in C). In contrast, no long-distance movement was observed with RA-GFP, suggesting that the same R-rich domain required for nucleolar localization and production of c-RNPs is essential for long-distance virus movement (Figure 3A–C) (single arginine substitutions did not affect nuclear localization and c-RNP formation and were able to rescue long-distance virus movement; Figure 3C). Similarly, no long-distance viral movement was observed with any leucine-rich region mutant (Figure 3A–C). The phenotype of the L149A mutation was further confirmed by inserting the same critical mutation into ORF3 of a full-length clone of pea enation mosaic virus-2 (PEMV-2), an umbravirus closely related to GRV, resulting in the complete blockage of long-distance movement of this virus (Figure 3D). Thus, the R- and L-rich regions are both required for long-distance viral movement and the mutations reveal a strong correlation between the localization of the ORF3 protein to the nucleolus, its capacity to form c-RNP with viral RNA and the ability of the virus to move through the plant (Figure 3C). The trafficking of the ORF3 protein to the nucleolus and ultimately to the cytoplasm is therefore key to successful GRV infection.

### *L149A-GFP protein accumulates in multiple CBLs*

To identify the small subnuclear bodies in which the L149A-GFP protein accumulates (Figure 1G), infection sites produced by L149A-GFP and ORF3-GFP were labelled with fluorescent (red) antibodies to the CB protein markers, coilin (*Arabidopsis thaliana* coilin—Atcoilin; Collier *et al*, 2006) and U2B″ (Beven *et al*, 1995; Boudonck *et al*, 1999) (Figure 4A and B). In control (healthy (data not shown) or infected with TMVΔCP-GFP (Figure 4A)) *N. benthamiana* cells, the antibodies detected usually one and up to three CBs. In contrast, in cells containing L149A-GFP, the antibodies colocalized with multiple subnuclear bodies showing L149A-GFP fluorescence (Figure 4A and B). The number of such bodies per cell was significantly increased (ca. 6–12) compared to control cells. Thus, the L149A-GFP mutant protein is unable to localize to the nucleolus and instead accumulates in multiple subnuclear structures, which contain CB marker proteins and therefore are termed here CBLs. In cells containing ORF3-GFP, the Atcoilin and U2B″ antibodies colocalized with ORF3 protein in the nucleolus, but unexpectedly did not detect any CBs (Figure 4A and B) in any of the 50 infected cells analysed in each of the five experiments. Thus, the ORF3 protein accumulates in the nucleolus and disrupts or alters CB integrity, relocalizing coilin and U2B″ to the nucleolus.

### *ORF3 protein causes CBLs to fuse with nucleoli*

To investigate the effect of expressing ORF3-GFP on CBs, its distribution in the nucleus was examined in a pseudo-time course of infection experiment. Virus infection spreads from the initial infected cell to generate a lesion on the leaf where the cells in the lesion are at different stages of infection (Figure 4C, left panel): cells at the leading edge of the growing (3 days post-inoculation) infection site represent

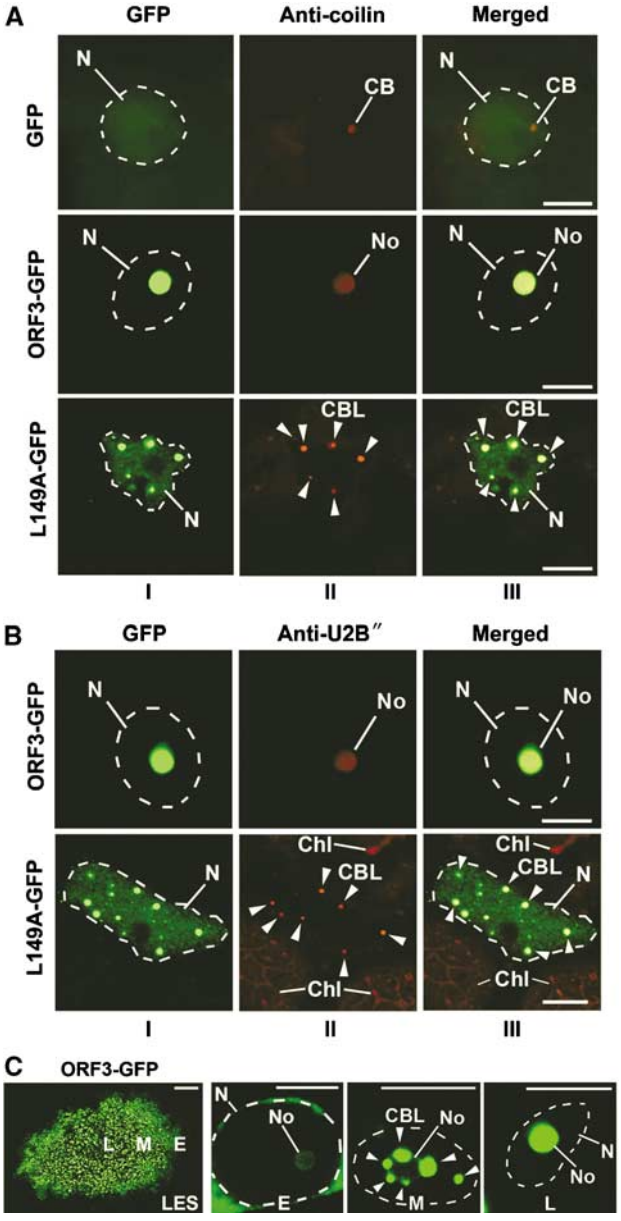


**Figure 4** Effect of ORF3 protein on the integrity and localization of CBs. (**A, B**) Confocal images of epidermal cells infected with TMVΔCP expressing ORF3-GFP, L149A-GFP and free GFP (as a control) and immunostained using antibodies to coilin (A) and U2B″ (B). In ORF3-GFP-infected cells, coilin and U2B″ localize with the ORF3 protein to nucleoli, whereas in L149A-GFP-infected cells, these proteins are found in multiple small bodies (CBLs). CBs are detected in GFP-expressing cells but not in ORF3-GFP cells. Panels: I—GFP images; II—fluorescent (red) antibody labelling; III—overlay images. CB, Cajal bodies; CBL, CB-like structures (shown by arrowheads); No, nucleoli; N, nuclei (indicated by dashed lines according to DAPI staining). Chl, chloroplasts showing natural red autofluorescence. Scale bars, 5 μm. (**C**) Intranuclear localization of the ORF3-GFP protein in a pseudo-time course of ORF3-GFP infection. The left panel (LES, for lesion) shows a GFP image of a whole virus-infected lesion with cells corresponding to different stages of infection. Cells at the front of the infection site represent early infection events (E), whereas those cells in the centre of the infection site represent late events (L). 'Early' event cells show fluorescence mainly in the perinuclear region; intermediate (middle) stage cells (M) show accumulation of fluorescence in multiple subnuclear bodies, similar to the CBLs that merge with the nucleolus at later stage (L). Scale bars, 5 μm, except for lesion in (C) (left panel)—200 μm.

early infection events whereas those cells in the centre of the infection site represent late events (Figure 4C). Three days after inoculation with ORF3-GFP, 'early' event cells showed fluorescence mainly in the perinuclear region with weak labelling of the nucleolus (Figure 4C). Intermediate (middle) stage cells showed significant accumulation of fluorescence in multiple subnuclear bodies, similar to the CBLs produced in the presence of the L149A mutant, that appeared to merge with the nucleolus such that, at later stages, only the nucleolus was intensely labelled (Figure 4C). Thus, it appears that after entering the nucleus, the ORF3 protein causes the reorganization of CBs into multiple structures (CBLs), which then fuse with the nucleolus. The L149A-GFP protein is still able to target and modify CBs but does not prompt their fusion with the nucleolus (Figure 4A and B), suggesting that L149 is critical to this function of the ORF3 protein.

### *Fusion of CBLs in GRV-infected plants*

To demonstrate that the modification of CBs and fusion of CBLs with the nucleolus was not an artefact of expression of the ORF3-GFP protein from a TMV vector, we determined the fate of CBs during native umbravirus (GRV) infection. The CB marker, Atcoilin, was fused to GFP (Atcoilin-GFP) and expressed from *A. tumefaciens* following agroinoculation of healthy *N. benthamiana* plants and plants preinfected with GRV containing YB satellite RNA (GRV-YB). This particular infection induces yellow blotch symptoms at the front of systemic infection and therefore acts as a visible marker of infection where cells ahead of, at and behind the advancing yellow blotch symptoms represent early, middle and late stages of infection, respectively (Figure 5A, left panel). Atcoilin fluorescence in cells at different stages in the development of umbravirus infection again showed multiple CBLs appearing to merge with the nucleolus, whereas in healthy cells, CBs remained distinct from the nucleolus (Figure 5A, right panel).

This was further confirmed by examining the localization of Atcoilin-GFP (a CB-specific marker) and *Arabidopsis* fibrillarin 2 (a nucleolar and CB marker) (Barneche *et al*, 2000) fused to monocistronic red fluorescent protein (AtFib2-mRFP), in healthy and GRV-infected plants co-infiltrated with *Agrobacterium* strains expressing the fusions. As expected, in healthy plants, AtFib2 labelled both the CBs (usually 1–3) and the nucleolus, whereas Atcoilin colocalized with AtFib2 only in CBs (Figure 5B). However, at early stages of GRV infection, AtFib2 labelled the nucleolus and colocalized with Atcoilin in multiple CBLs, which later merged with the nucleolus (Figure 5B). Thus, reorganization of CBs and fusion of CBLs with the nucleolus occur both when ORF3 is expressed from a TMV vector and in a native GRV infection.

### *Fibrillarin is present in c-RNPs*

In addition to the nuclear events described in Figures 4 and 5, at the later stages of infection (when cRNP inclusions are formed), fibrillarin was also detected in cRNP-containing inclusions in the cytoplasm of cells expressing ORF3-GFP (Figure 6A). Where the c-RNPs showed sub-structure (as in Figure 6A), anti-fibrillarin antibody colocalized with ORF3-GFP fluorescence both in the nucleolus and in the general diffuse labelling and punctuate bodies in the c-RNPs (Figure 6A). In contrast, in healthy plants or plants expressing GFP alone following infection with TMVΔCP-GFP,

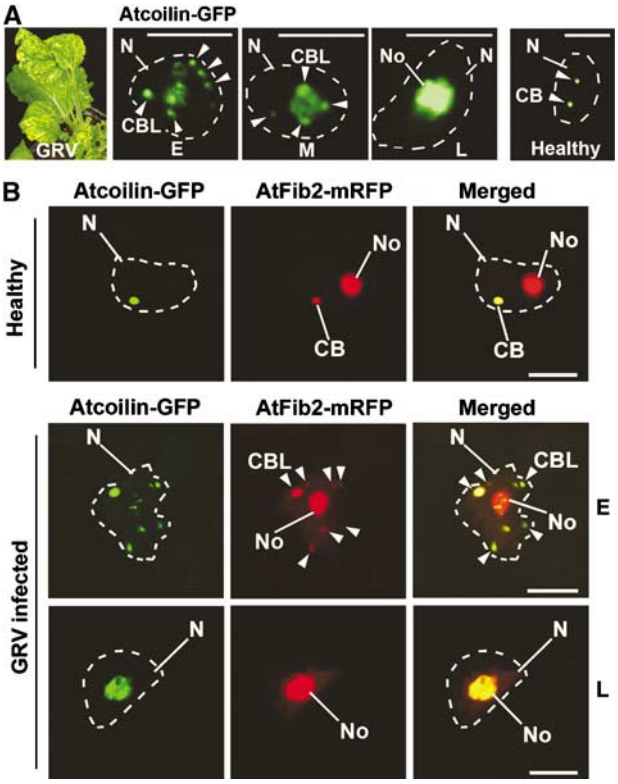


**Figure 5** Fusion of CBLs with the nucleolus in GRV-infected plants. (**A**) Localization of Atcoilin-GFP delivered by *Agrobacterium* in a pseudo-time course of GRV-YB infection from early (E), middle (M) and late (L) stages of the infection compared to a healthy cell. GRV-YB infection induces yellow blotch symptoms (left panel) at the front of systemic infection and therefore acts as a visible marker of infection progression. Atcoilin-GFP fluorescence in cells at different stages of GRV infection shows multiple CBLs merging with the nucleolus, whereas in healthy cells, CBs remains distinct from the nucleolus (right panel). (**B**) Subnuclear colocalization of Atcoilin-GFP and AtFib2-mRFP delivered by *Agrobacterium* into healthy or GRV-YB—infected plant cells at early (E) and late (L) stages of GRV infection. In healthy plant cells, AtFib2 labels both the CBs (usually 1–3 per nucleus) and the nucleolus, whereas Atcoilin colocalizes with AtFib2 only in CBs. At early stages of GRV infection (E), AtFib2 colocalizes with Atcoilin in multiple CBLs, which merge with the nucleolus at late stage (L). CB, Cajal bodies; CBL, CB-like structures (shown by arrowheads); No, nucleoli; N, nuclei (shown by dashed lines according to DAPI staining). Scale bars, 5 μm.

anti-fibrillarin antibody labelled only nucleoli and CBs (Figure 6A). Likewise, the mutants RA-GFP (defective in nuclear/nucleolar import), L152A-GFP/L153A-GFP (defective in nuclear export) and L149A-GFP (defective in nucleolar localization and nuclear export) only formed c-PAs, which did not contain fibrillarin (Figure 6A). Thus, the presence of the normally nuclear fibrillarin in cytoplasmic inclusions was dependent on wild-type ORF3 protein and the formation of viral RNPs.

To demonstrate that nucleolar to cytoplasmic redistribution of some fibrillarin also occurs during native GRV infection, an AtFib2-GFP fusion was introduced into *N. benthamiana* plants infected with GRV-YB as described above. In healthy plants, the AtFib2-GFP labelled nucleoli and CBs (Figure 6B). However, in infected plants, at late stages of infection, fluorescence was observed in nucleoli and c-RNPs, but not CBs (Figure 6C). Further support that c-RNPs contain both RNP particles and fibrillarin was obtained by IGL using antibodies against the ORF3 protein and fibrillarin (Supplementary Figure S1A, panels I and II) and from copurification of fibrillarin with RNP complexes in a $Cs_2SO_4$ density gradient (Supplementary Figure S1B–D), suggesting that fibrillarin may be involved in the formation of the c-RNPs.

The unusual localization of fibrillarin, mediated by the ORF3 protein, does not reflect increased fibrillarin production in the GRV-infected and ORF3-expressing cells. Similar amounts of fibrillarin were observed in cells infected with GRV, ORF3-GFP, all its mutants and the control healthy cells by Western blot analysis (Supplementary Figure S2) and by comparison of levels of red fluorescence characteristic of anti-fibrillarin antibodies within cells expressing all tested ORF3 constructs (Supplementary Table SI; also see for details legends for Figure 6A and B). Thus, the ORF3 protein mediates partial redistribution of fibrillarin from the nucleolus to the cytoplasm (and into cytoplasmic inclusions) only if the ORF3 protein itself is able first to enter the nucleus/nucleolus and then exit to the cytoplasm.

## Discussion

Here, we demonstrate that the GRV ORF3 long-distance movement protein traffics to the nucleolus via a mechanism involving the reorganization of CBs and their fusion with the nucleolus. Nucleolar localization and trafficking of ORF3 protein from the nucleolus to the cytoplasm are essential for the umbravirus infection. The integral connection between nucleolar targeting of the ORF3 protein and its biological function in virus long-distance spread is demonstrated by mutations in the R- and L-rich domains that block nucleolar localization or nuclear export of the ORF3 protein, and which prevent the formation of cytoplasmic viral RNPs and their long-distance movement. We provide a model whereby the ORF3 protein may hijack some elements of trafficking pathways involving CBs and the nucleolus before redistribution to cytoplasmic inclusion bodies and the formation of viral RNPs that are capable of long-distance movement (Figure 7). These processes are likely to require interactions between the ORF3 protein and different host proteins at different stages of infection, and we have initial evidence for the involvement of the major nucleolar protein, fibrillarin, in viral RNP formation (Kim *et al*, in preparation). This model demonstrates novel functions for plant CBs and the nucleolus in the viral life cycle.

After entering the plant cell, GRV establishes the translation and replication of viral RNA. Once the ORF3 protein has been translated, it enters the nucleus and targets and reorganizes CBs into multiple CBLs (Figure 7). The mechanisms by which the ORF3 protein targets CBs and produces CBLs are unknown. Targeting of CBs by the ORF3 protein may use elements of existing CB-trafficking pathways. For example, part of the maturation pathway of snRNPs in mammalian cells occurs in the cytoplasm and involves a complex containing the survival of motor neurons (SMN) protein, which together with the snRNP are re-imported into the nucleus and targeted to CBs (Sleeman and Lamond, 1999; Navascues *et al*, 2004; Matera and Shpargel, 2006). Particular snRNP proteins contain modified (symmetric di-methyl) arginines (sDMAs), which enhance the formation of snRNPs and interaction with SMN (Paushkin *et al*, 2002). In preliminary experiments, we have identified sDMAs in the ORF3 protein,

suggesting that targeting of the ORF3 protein to CBs could involve interactions with the SMN protein. Although SMN protein has yet to be identified in plants, the existence of an orthologue has been suggested (Collier *et al*, 2006).

The formation of CBLs may involve either fragmentation of CBs into multiple bodies by the ORF3 protein or the redistribution of CB components into new structures containing the ORF3 protein. Interestingly, the multiple CBL phenotype, described here, is similar to that of the *poly Cajal bodies* (*pcb*) mutant of *Arabidopsis* (Collier *et al*, 2006). As the protein normally encoded by this, as yet unidentified, gene appears to regulate CB formation, ORF3 protein may interfere with the function of this or other proteins to affect the integrity and number of CBs in nuclei. The second possibility is that the ORF3 protein causes the redistribution of CB components, such as coilin, U2B″ and fibrillarin, to form CBLs along with the ORF3 protein.

ORF3 protein trafficking to the nucleolus uses a novel pathway of nucleolar import by causing the fusion of CBLs with the nucleolus. The physical and functional association of the nucleolus and CBs is well documented and is controlled by complex molecular interactions among CB and nucleolar proteins such as coilin, SMN, fibrillarin and Nopp140 (Ogg and Lamond, 2002; Cioce and Lamond, 2005). Expression of mutant versions of some of these proteins has profound effects on CB structure and function, causing disruption or dispersal and compositional changes (Jones *et al*, 2001; Pellizzoni *et al*, 2001; Tucker *et al*, 2001). Moreover, phosphorylation of coilin is an important factor determining physical interactions and trafficking of CBs (Ogg and Lamond, 2002; Cioce and Lamond, 2005). For example, CBs form within the nucleolus of HeLa cells upon treatment with okadaic acid (an inhibitor of protein phosphatase) and with transient expression of coilin mutated at a single serine residue (Lyon *et al*, 1997; Sleeman *et al*, 1998). CBs have also been observed within nucleoli in human breast carcinomas (Ochs *et al*, 1994) and in liver cells of hibernating dormice (Malatesta *et al*, 1994). Therefore, the ORF3 protein may interfere with normal protein–protein interactions or post-translational modifications causing the reorganization and fusion of CBs with the nucleolus.

Previously, we have shown that the umbraviral RNP particles are the form of the virus that moves viral RNA long distances through the phloem, and are therefore, essential for umbravirus systemic infection (Taliansky *et al*, 2003). Umbraviral RNP assembly occurs in the cytoplasm (Taliansky *et al*, 2003) such that the last stage of the nuclear voyage of the ORF3 protein is its nuclear export leading to formation of virus RNP particles in cytoplasmic inclusions. Viral RNP production occurs only if the ORF3 protein has first been localized to the nucleolus, suggesting that it recruits some nucleolar factor(s) for this process. One possible candidate is fibrillarin, an RNA-binding protein, which colocalizes with the ORF3 protein in c-RNPs, even though it does not normally accumulate in the cytoplasm. Thus, fibrillarin must either be

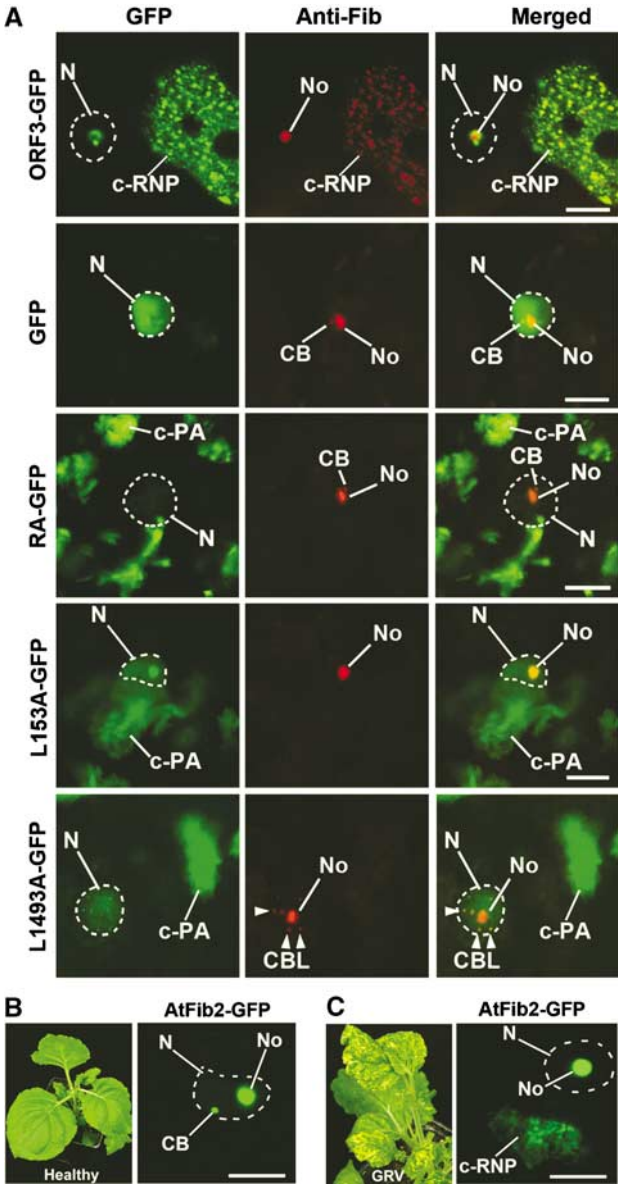


**Figure 6** Relocalization of fibrillarin from the nucleolus to cytoplasm in *N. benthamiana* cells at late stages of infection. (**A**) Intracellular localization of fibrillarin in cells of leaves inoculated with TMVΔCP expressing ORF3-GFP, GFP alone, RA-GFP, L149A-GFP and L153A-GFP at late stages of infection (7 days post-inoculation). Partial cell images are shown to include nucleus and cytoplasmic inclusions when present. Fibrillarin was immunostained with fluorescent (red) antibody. Left-hand panel—GFP images; centre panel—fluorescent (red) antibody labelling; right-hand panel—overlay images. In leaves infected with ORF3-GFP, anti-fibrillarin antibody labels nucleoli and cytoplasmic inclusions (c-RNPs). In cells expressing GFP alone or any of the mutants, anti-fibrillarin antibody labels only nucleoli, CBs or CBLs (L149A-GFP) but no structures in the cytoplasm. The overall red fluorescence levels (emitted by anti-fibrillarin antibodies) within cells expressing all tested ORF3 constructs were essentially similar (see Supplementary Table SI). However, in the ORF3-GFP image presented in this figure, the gain was increased to show the cytoplasmic (c-RNP) localization of fibrillarin accumulation more clearly. For other constructs (GFP alone, RA-GFP, L149A-GFP and L153A-GFP) increasing the gain did not reveal any fibrillarin accumulation in the cytoplasm. (**B, C**) Localization of AtFib2-GFP delivered by *Agrobacterium* into healthy cells (B) or GRV-YB-infected cells at a late stage of infection (C). In healthy cells, the AtFib2-GFP labels nucleoli and CBs (image shows the nucleus containing a single CB). In cells of the leaves inoculated with GRV-YB (7 days post-inoculation), fluorescence is observed in nucleoli and c-RNPs, but not CBs. N, nucleus (shown by dashed lines); No, nucleolus, CB, Cajal bodies; CBL, CB-like structures (shown by arrowheads); c-RNP, cytoplasmic RNP complexes; c-PA, cytoplasmic protein aggregates. Scale bars, 5 μm.

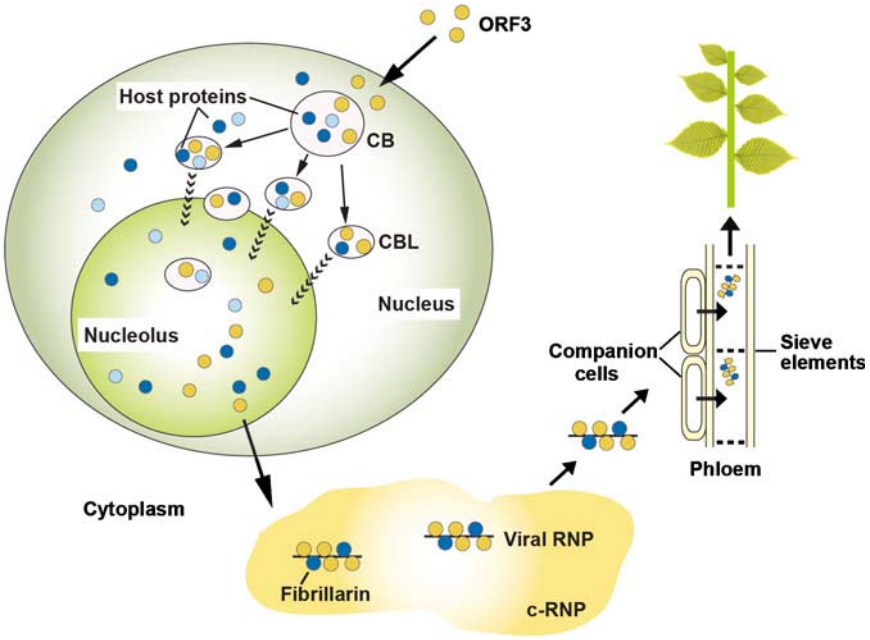


**Figure 7** Model of GRV infection and the role of ORF3 protein, fibrillarin, CBs and the nucleolus. Upon GRV infection, the ORF3 protein is produced in the cytoplasm and is targeted to CBs reorganizing them into multiple CBLs. The CBLs then move to and fuse with the nucleolus by an unknown mechanism. Host proteins are likely to be involved in targeting of the ORF3 protein to the CBs, reorganizing CBs and causing their fusion with the nucleolus. One such host protein is fibrillarin and the ORF3 protein causes the relocalization of some of the nuclear/nucleolar fibrillarin pool to the cytoplasm where viral RNPs containing the ORF3 protein, fibrillarin and viral RNA accumulate. When produced in companion cells, the viral RNPs are able to migrate into the phloem sieve elements where they are transported to the rest of the plant to generate a systemic infection. Orange circles—the ORF3 protein; dark blue circles—fibrillarin, light blue circles—other host proteins including coilin and U2B″.

retained in the cytoplasm after its translation by interaction with cytoplasmic ORF3 protein or c-RNPs or actively redistributed from the nucleolus to the cytoplasm along with the ORF3 protein. The latter possibility is more likely because neither the L149A and L153A mutants (defective in nuclear export) nor the RA mutant, which is defective in nuclear import and accumulates only in the cytoplasm, caused relocalization of fibrillarin to the cytoplasmic inclusions. In addition to colocalizing with c-RNP, fibrillarin was copurified with umbraviral RNP particles and therefore it may be directly involved in their formation. In agreement with this suggestion, we recently demonstrated that *in vitro*, fibrillarin is able to interact with the ORF3 protein and promote formation of filamentous RNP particles with structural properties similar to *in vivo* RNP complexes (Kim *et al*, in preparation). It is also worth noting that relocalization of fibrillarin to the cytoplasm occurs at the late stages of viral infection when viral RNP particles start to form within cRNPs and move through the phloem. Finally, when formed in phloem companion cells, the viral RNPs are able to enter sieve elements and move through the plant to cause systemic infection.

How the ORF3 protein reprogrammes nuclear trafficking pathways and molecular interactions for successful infection will have implications for other plant and animal viruses that interact with the nucleolus, and will aid our understanding of interactions that occur between the nucleolus, CBs and their components. The challenges for the future are to identify the host proteins that interact with the ORF3 protein and target it to CBs, mediating the reorganization of CBs, their fusion to the nucleolus and participation in viral RNP formation, long-distance movement and infection.

## Materials and methods

### *Virus strains and TMV-based constructs*

GRV-YB was maintained as a stock isolate by repeated passages in *N. benthamiana* plants. The PEMV-2 infectious cDNA clone was described by Ryabov *et al* (2001). The TMV infectious clone expressing GRV ORF3 instead of TMV CP (TMVΔCP.ORF3) (Ryabov *et al*, 1999) was used to generate a vector encoding the ORF3 protein fused to the N-terminus of GFP (TMVΔCP.ORF3-GFP; Figure 1B) by overlap PCR using self-complementary primers corresponding to the 16 3′-terminal nucleotides of ORF3 and the first 13 nucleotides of the GFP gene. Changes were introduced into ORF3 coding sequences of the constructs TMVΔCP.ORF3-GFP to produce mutants listed in Figure 1A by PCR using self-complementary mutagenic primers. Preparation of DNA templates, *in vitro* RNA transcription using the mMessage mMachine T7 kit (Ambion) and inoculation of plants were as described by Ryabov *et al* (1999).

### *Generation and Agrobacterium-mediated expression of constructs encoding markers of the nucleolus and CBs*

pROK2 binary vectors, derivatives of pBIN19 (Bevan, 1984), expressing GFP or mRFP were converted into a Gateway Destination vector by inserting a Gateway cassette according to the manufacturer's instruction (Invitrogen) to generate pROK2.GFPattR and pROK2.mRFPattR, respectively. cDNA clones encoding *A. thaliana* coilin and fibrillarin were amplified by PCR and inserted into these Destination vectors. The recombinant plasmids were electroporated into *A. tumefaciens* (GV3101). Transient expression of the constructs was achieved by infiltration of the *Agrobacterium* to the underside of a *N. benthamiana* leaf.

### *Imaging analysis*

Localization of GFP and mRFP fusion proteins was monitored using TCS SP2 (Leica Microsystems) and MRC 1000 (Bio-Rad) confocal laser scanning microscopes. To locate nuclei precisely, the leaf tissues were infiltrated with phosphate-buffered saline containing 1 μg/ml 4′,6′-diamidino-2-phenylindole (DAPI). Endogenous coilin, U2B″ and fibrillarin were localized using primary rabbit antibodies

to Atcoilin and U2B″, and primary mouse monoclonal antibody to human fibrillarin (Cytoskeleton Inc.). The primary antibodies were visualized by Alexa Fluor 568 (red)- or 488 (green)-conjugated anti-mouse or anti-rabbit secondary antibodies (Molecular Probes).

#### *Electron microscopy, IGL and ISH*

Pieces of leaf material infected with derivatives of TMVΔCP.ORF3-GFP were sampled 7–10 days post-inoculation, fixed, embedded and sectioned (Taliansky *et al*, 2003). Samples were incubated with anti-ORF3 protein antibodies (for IGL) and specific digoxigenin-labelled GRV ORF3 RNA probes (for ISH), visualized by antibodies conjugated to gold particles and stained essentially as described before (Taliansky *et al*, 2003) and examined under a Phillips CM 10 electron microscope.

#### *Analysis of virus accumulation: infectivity tests and RNA analysis*

Virus infectivity in samples from inoculated and uninoculated leaves infected with derivatives of TMVΔCP.ORF3-GFP and GRV was assessed by counting the number of lesions induced in half leaves of *N. tabacum* 'Xanthi-nc' and *C. quinoa* plants, respectively. Total RNA was extracted from plants using RNAwiz solution (Ambion). RT–PCR analysis of the accumulation of RNA of TMVΔCP.ORF3-GFP derivatives was performed using primer combinations corresponding to a GFP gene fragment (270 nt in length) and a fragment of the ubiquitin gene (176 nt) as a control. First strand cDNAs were synthesized using the reverse primers and SuperScript reverse transcriptase (Invitrogen) according to the manufacturer's recommendations and used as templates for PCR amplification through 25–50 cycles. Northern blot analysis of GRV RNA was performed with $^{32}$P-labelled cDNA probe corresponding to the clone gr21GRV as described by Taliansky *et al* (1996).

#### *Print hybridization*

For the print hybridization assay, leaves were press-blotted to Hybond N membrane that had been presoaked with 50 mM NaOH containing 2.5 mM EDTA and dried as described by Ryabov *et al* (2001). The probe was $^{32}$P-labelled cDNA corresponding to PEMV-2 ORF3.

The nucleotide sequence of the NbFib cDNA was deposited in GenBank with accession no. AM269909.

#### *Supplementary data*

Supplementary data are available at *The EMBO Journal* Online (http://www.embojournal.org).

## Acknowledgements

We thank P Shaw (JIC, Norwich, UK) for providing the Atcoilin cDNA clone and antibodies to Atcoilin and U2B″ and M Echeverria (Université de Perpignan, Perpignan, France) for the AtFib2 cDNA clone. This work was supported by grant-in-aid from the Scottish Executive Environment and Rural Affairs Department, by the Royal Society (JWSB, NOK and MT), BBSRC (EVV), INTAS (fellowship to DVR) and the Russian Foundation for Basic Research (NOK).

## References

Barneche F, Steinmetz F, Echeverria M (2000) Fibrillarin genes encode both a conserved nucleolar protein and a novel small nucleolar RNA involved in ribosomal RNA methylation in *Arabidopsis thaliana*. *J Biol Chem* **275:** 27212–27220

Bevan M (1984) Binary *Agrobacterium* vectors for plant transformation. *Nucleic Acids Res* **12:** 8711–8721

Beven AF, Simpson GG, Brown JWS, Shaw PJ (1995) The organization of spliceosomal components in the nuclei of higher plants. *J Cell Sci* **108:** 509–518

Boudonck K, Dolan L, Shaw P (1999) Coiled body numbers in the *Arabidopsis* root epidermis are regulated by cell type, developmental stage and cell cycle parameters. *J Cell Sci* **111:** 3687–3694

Cioce M, Lamond AI (2005) Cajal bodies: a long history of discovery. *Annu Rev Cell Dev Biol* **21:** 105–131

Collier S, Pendle A, Boudonck K, van Rij T, Dolan L, Shaw PJ (2006) A distant coilin homologue is required for the formation of Cajal bodies in *Arabidopsis*. *Mol Biol Cell* **17:** 2942–2951

Esau K, Cronshaw J (1967) Relation of tobacco mosaic virus with host cells. *J Cell Biol* **33:** 665–678

Hiscox JA (2002) The nucleolus—a gateway to viral infection? *Arch Virol* **147:** 1077–1089

Hiscox JA (2007) RNA viruses:hijacking the dynamic nucleolus. *Nat Rev Microbiol* **5:** 119–127

Hull R (2002) *Mathews' Plant Virology*. London, UK: Academic Press Ltd

Jones KW, Gorzynski K, Hales CM, Fischer U, Badbanchi F, Terns RM, Terns MP (2001) Direct interaction of the spinal muscular atrophy disease protein SMN with the small nucleolar RNA-associated protein fibrillarin. *J Biol Chem* **276:** 38645–38651

Li CF, Pontes O, El-Shami M, Henderson IR, Bernatavichute YV, Chan SW-L, Lagrange T, Pikaard CS, Jacobsen SE (2006) An ARGONAUTE4-containing nuclear processing center colocalized with Cajal bodies in *Arabidopsis thaliana*. *Cell* **126:** 93–106

Lyon CE, Bohmann K, Sleeman J, Lamond AI (1997) Inhibition of protein dephosphorylation results in the accumulation of splicing snRNPs and coiled bodies within the nucleolus. *Exp Cell Res* **230:** 84–93

Malatesta M, Zancanaro C, Martin TE, Chan EK, Amalric F, Luhrmann R, Vogel P, Fakan S (1994) Cytochemical and immunocytochemical characterization of nuclear bodies during hibernation. *Eur J Cell Biol* **65:** 82–93

Matera AG, Shpargel KB (2006) Pumpimg RNA: nuclear bodybuilding along the RNP pipeline. *Curr Opin Cell Biol* **18:** 317–324

Navascues J, Berciano MT, Tucker KE, Lafarga M, Matera AG (2004) Targeting SMN to Cajal bodies and nuclear gems during neuritogenesis. *Chromosoma* **112:** 398–409

Ogg SC, Lamond AI (2002) Cajal bodies and coilin-moving towards function. *J Cell Biol* **159:** 17–21

Olsen MOJ (2004) Nontraditional roles of the nucleolus. In *The Nucleolus*, Olsen MOJ (ed) pp 329–342. New York, USA: Landes; Georgetown, USA: Kluwer

Ochs RL, Stein Jr TW, Tan EM (1994) Coiled bodies in the nucleolus of breast cancer cells. *J Cell Sci* **107:** 385–399

Paushkin S, Gubitz AK, Massenet S, Dreyfuss G (2002) The SMN complex, an assemblysome of ribonucleoproteins. *Curr Opin Cell Biol* **14:** 305–312

Platani M, Goldberg I, Lamond AI, Swedlow JR (2002) Cajal bodies dynamics and association with chromatin are ATP-dependent. *Nat Cell Biol* **4:** 502–508

Pellizzoni L, Baccon J, Charroux B, Dreyfuss G (2001) The survival of motor neurons (SMN) protein interacts with the snoRNP proteins fibrillarin and GAR1. *Curr Biol* **11:** 1079–1088

Pontes O, Li CF, Nunes P C, Haag J, Ream T, Vitins A, Jacobsen SE, Pikaard CS (2006) The *Arabidopsis* chromatin-modifying nuclear siRNA pathway involves a nucleolar RNA processing center. *Cell* **126:** 79–92

Rubbi CP, Milner J (2003) Disruption of the nucleolus mediates stabilization of p53 in response to DNA damage and other stresses. *EMBO J* **22:** 6068–6077

Ryabov EV, Fraser G, Mayo MA, Barker H, Taliansky M (2001) Umbravirus gene expression helps potato leafroll virus to invade mesophyll tissues and to be transmitted mechanically between plants. *Virology* **286:** 363–372

Ryabov EV, Kim SH, Taliansky ME (2004) Identification of a nuclear localization signal and nuclear export signal of the umbraviral long-distance RNA movement protein. *J Gen Virol* **85:** 1329–1333

Ryabov EV, Oparka KJ, Santa Cruz S, Robinson DJ, Taliansky ME (1998) intracellular location of two groundnut rosette umbravirus proteins delivered by PVX and TMV vectors. *Virology* **242:** 303–313

Ryabov EV, Robinson DJ, Taliansky ME (1999) A plant virus-encoded protein facilitates long-distance movement of heterologous viral RNA. *Proc Natl Acad Sci USA* **96:** 1212–1217

Sleeman JE, Ajuh P, Lamond AI (2001) snRNP protein expression enhances the formation of Cajal bodies containing p80-coilin and SMN. *J Cell Sci* **114:** 4407–4419

 

Sleeman JE, Lamond AI (1999) Newly assembled snRNPs associate with coiled bodies before speckles, suggesting a nuclear snRNP maturation pathway. *Curr Biol* **9:** 1065–1074

Sleeman JE, Lyon CE, Platani M, Kreivi JP, Lamond AI (1998) Dynamic interactions between slicing snRNPs, coiled bodies and nucleoli revealed using snRNP protein fusions to the green fluorescent protein. *Exp Cell Res* **243:** 290–304

Taliansky ME, Roberts IM, Kalinina N, Ryabov EV, Raj SK, Robinson DJ, Oparka KJ (2003) An umbraviral protein, involved in long-distance RNA movement, binds viral RNA and forms unique, protective ribonucleoprotein complexes. *J Virol* **77:** 3031–3040

Taliansky ME, Robinson DJ, Murant AF (1996) Complete nucleotide sequence and organization of the RNA genome of groundnut rosette umbravirus. *J Gen Virol* **77:** 2335–2345

Taliansky ME, Robinson DJ (2003) Molecular biology of umbraviruses: phantom warriors. *J Gen Virol* **84:** 1951–1960

Tucker KE, Berciano MT, Jacobs EY, LePage DF, Shpargel KB, Rossire JJ, Chan EK, Lafarga M, Conlon RA, Matera AG (2001) Residual Cajal bodies in coilin knockout mice fail to recruit Sm snRNPs and SMN, the spinal muscular atrophy gene product. *J Cell Biol* **154:** 293–307